



## Modeling the Transmission Dynamics and Stability of Nipah Virus

Mamta Kumari

**ABSTRACT:** Nipah virus (NiV) is a zoonosis characterized by high transmission and death rates. Existing SIR, SEIR and SIRD-type models mainly focus on transmission from living infectious individuals and from dead bodies of infected persons that are not handled safely. The SEIR model by Lakshmi and Sabarmathi, though, does not include disease-induced mortality or corpse-mediated transmission, which may lead to results, such as an overestimation of the epidemic peak and an underestimation of the outbreak duration. In this work, the existing framework is extended by the addition of an infectious deceased compartment. An SEIRD model is developed that considers both direct human-to-human and corpse-mediated transmission. Estimations of parameters are taken from recent outbreaks, and the basic reproduction number,  $\mathcal{R}_D$ , is derived analytically. Python programs are used for mathematical simulations. The results show that when corpse-mediated transmission is included, the projected epidemic peak is lower, and there is a delay in the time to reach the peak. The model also provides a better estimate of the total outbreak size compared to the classical SEIR model. Sensitivity analysis using partial rank correlation coefficients (PRCC) shows that direct transmission ( $\beta_1$ ) and corpse removal rate ( $\omega$ ) are the most influential parameters. The SEIRD model, by including postmortem transmission, matches observed outbreak patterns more closely and highlights the need to combine isolation with safe burial practices to control NiV epidemics.

**Keywords:** Nipah virus, SEIRD model, reproduction number, stability, corpse-mediated transmission.

### Contents

<b>1 Introduction</b>	<b>2</b>
<b>2 Model Formulation</b>	<b>2</b>
<b>3 SEIRD Model Equations</b>	<b>4</b>
<b>4 Equilibria and Stability Analysis</b>	<b>4</b>
4.1 Disease-Free Equilibrium and Feasible Region . . . . .	4
4.2 Stability Analysis of the Disease-Free Equilibrium (DFE) . . . . .	5
4.3 Existence of Endemic Equilibrium . . . . .	6
<b>5 Global Stability of the Disease-Free Equilibrium</b>	<b>7</b>
<b>6 Numerical Simulations and Comparison</b>	<b>8</b>
<b>7 Interpretation and Sensitivity Analysis of the SEIRD Model</b>	<b>9</b>
7.1 Sensitivity Analysis . . . . .	10
7.2 Phase Plane Analysis . . . . .	12
<b>8 Contour Plot of Reproduction Number <math>\mathcal{R}_D</math></b>	<b>13</b>
<b>9 Conclusion</b>	<b>13</b>
<b>10 Future Scope</b>	<b>14</b>

---

2020 *Mathematics Subject Classification:* 34D05, 34A34, 92D30, 92C60.

Submitted November 27, 2025. Published March 14, 2026

## 1. Introduction

Nipah virus (NiV) is a deadly zoonotic pathogen responsible for frequent outbreaks mainly in the southern and southeastern regions of Asia, including Bangladesh and India, where the fatality rate ranges from 40-75% [1,2,3]. NiV is classified as a zoonosis [4,5] and is characterized by high transmission and death rates [1,6]. The main mode of transmission is human-to-human contact, but other cultural practices such as care-giving and funeral rituals further increase the spread [7,8]. Therefore, understanding NiV dynamics is important for planning effective interventions, and mathematical modeling is one of the useful methods [9,10]. Most researchers have used compartmental epidemic models [11] to study NiV transmission. SEIR-type approaches [12,13,14] and SIRD-type models [15] have been used to analyze transmission mechanisms and to identify isolation of individuals as a main strategy for controlling the disease [16,17,18]. Existing SEIR-type models mainly concentrate on transmission from living infectious individuals ( $I$ ) [12,13,14]. However, epidemiological studies have also indicated that there is significant transmission risk from dead bodies of infected persons that are not handled safely [7,6]. Despite this evidence, in most of these models, it is assumed that the disease spreads only through infected individuals ( $I$ ), without considering transmission through the dead bodies of individuals who have died from the infection. As a result, classical SEIR models, including that of Lakshmi and Sabarmathi [14], tend to overestimate the epidemic peak and underestimate the outbreak duration, thereby limiting the evaluation of control measures such as safe burial practices. In this work, this limitation is addressed by introducing an additional variable for deceased but unburied individuals ( $D_c$ ). This leads to an SEIRD model in which both living infectious individuals and corpses contribute to new infections. The basic reproduction number,  $\mathcal{R}_D$ , includes separate terms for direct and corpse-mediated transmission, providing a better assessment of outbreak potential [19,20,21]. Simulation and sensitivity analyses show that incorporating corpse-mediated transmission delays the occurrence of the epidemic peak, lowers its magnitude, and reduces the total number of cases compared to SEIR estimates. These results highlight that corpse removal, safe burial practices, and targeted interventions play a crucial role in controlling NiV outbreaks. Consequently, the SEIRD framework provides a more realistic and practical tool for outbreak assessment and control.

## 2. Model Formulation

The SEIRD compartmental model is used to analyze the spread of NiV. The total population is divided into five compartments, which are as follows:

1.  $S_c$  - This variable indicates the **susceptible individuals** who are at risk of contracting NiV.
2.  $E_c$  - This variable indicates the **exposed individuals** who have come into contact with infected individuals but are not yet showing any symptoms.
3.  $I_c$  - This variable indicates the **infected individuals** .
4.  $R_c$  - This variable indicates the **recovered individuals** who have recovered from the illness.
5.  $D_c$  - This variable represents **deceased individuals** whose remains have not yet been buried or handled with appropriate care

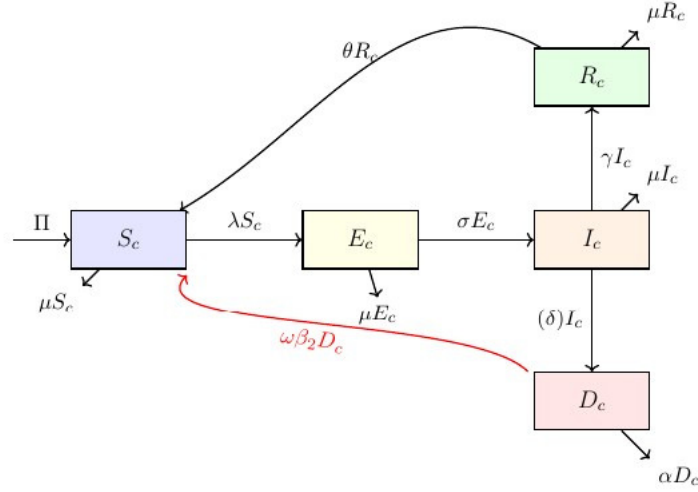


Figure 1: Flow chart of the SEIRD model for Nipah virus

In this study, a homogeneous population is presumed, in which each individual is equally likely to contract the disease through contact with infectious or deceased infected individuals.

Table 1 presents a summary of the models' variables and parameters, together with their epidemiological meanings.

Symbol	Description
$S_c(t)$	Number of susceptible individuals at time $t$
$E_c(t)$	Number of exposed individuals (in the incubation period) at time $t$
$I_c(t)$	Number of infectious individuals at time $t$
$R_c(t)$	Number of recovered individuals at time $t$
$D_c(t)$	Number of unburied deceased individuals at time $t$
$N(t)$	Total living population at time $t$ , $N = S_c + E_c + I_c + R_c$
$\Pi$	Constant recruitment rate
$\lambda$	Force of infection, incorporating contributions from both infectious and deceased individuals
$\beta_1$	Transmission rate from infectious individuals to susceptibles
$\beta_2$	Transmission rate from improperly handled corpses to susceptibles
$\sigma$	Rate of progression from exposed to infectious class (inverse of the incubation period)
$\gamma$	Recovery rate of infectious individuals
$\delta$	Disease-induced mortality rate among infectious individuals
$\mu$	Natural death rate (unrelated to NiV)
$\alpha$	Burial or safe disposal rate of deceased individuals
$\theta$	Rate of waning immunity, returning recovered individuals to the susceptible class
$\omega$	Proportion of corpses not safely handled, contributing to secondary infections

Table 1: Parameters and variables of the SEIRD model, along with their epidemiological interpretations.

The force of infection,  $\lambda$ , is given by

$$\lambda = \frac{\beta_1 I_c(t)}{N(t)} + \frac{\omega \beta_2 D_c(t)}{N(t)}, \quad (2.1)$$

and represents the rate at which susceptible individuals contract the infection. In this model,  $I_c(t)$  denotes

the number of infectious individuals,  $D_c(t)$  denotes the number of unburied deceased individuals,  $N(t)$  is the total number of living individuals, and  $\omega$  represents the proportion of deceased individuals that contribute to secondary transmission.

### 3. SEIRD Model Equations

The following system of ordinary differential equations governs the time-based dynamics of the SEIRD model, using the variables and parameters defined in Section 2.

$$\begin{aligned}
\frac{dS_c}{dt} &= \Pi - (\lambda + \mu)S_c + \theta R_c, \\
\frac{dE_c}{dt} &= \lambda S_c - (\sigma + \mu)E_c, \\
\frac{dI_c}{dt} &= \sigma E_c - (\gamma + \delta + \mu)I_c, \\
\frac{dR_c}{dt} &= \gamma I_c - (\mu + \theta)R_c, \\
\frac{dD_c}{dt} &= \delta I_c - \alpha D_c,
\end{aligned} \tag{3.1}$$

## 4. Equilibria and Stability Analysis

### 4.1. Disease-Free Equilibrium and Feasible Region

The state in which there is no infection is represented by the *disease-free equilibrium (DFE)* of system (3.1). Initially, it is confirmed that all solutions are non-negative so that the biological accuracy of the model is ensured.

**Theorem 4.1 (Non-negativity of Solutions)** *Consider the SEIRD system (3.1) subject to the following initial conditions*

$$S_c(0) = S_0 > 0, \quad E_c(0) = E_0 \geq 0, \quad I_c(0) = I_0 \geq 0, \quad R_c(0) = R_0 \geq 0, \quad D_c(0) = D_0 \geq 0.$$

Then, for all  $t \geq 0$ , the solution path

$$\{S_c(t), E_c(t), I_c(t), R_c(t), D_c(t)\}$$

remains non-negative.

**Remark 4.1** *Throughout the epidemic, this theorem ensures that the results of variables in every compartment maintain their biological significance.*

The feasible region for the model is

$$\Omega = \left\{ (S_c, E_c, I_c, R_c, D_c) \in \mathbb{R}_{\geq 0}^5 \mid S_c + E_c + I_c + R_c = N \leq \frac{\Pi}{\mu}, D_c \leq \frac{\delta}{\alpha} \cdot \frac{\Pi}{\mu} \right\}.$$

The set  $\Omega$  is shown to be positively invariant, meaning that any solution starting in  $\mathbb{R}_{\geq 0}^5$  ultimately moves into  $\Omega$  and remains restricted within it.

Assume that  $N(t) = S_c(t) + E_c(t) + I_c(t) + R_c(t)$  is the total number of living individuals. Then,

$$\frac{dN}{dt} = \Pi - \mu N - \delta I_c \leq \Pi - \mu N$$

is obtained by adding the first four equations of system (3.1).

By integrating this inequality, we obtain

$$N(t) \leq \frac{\Pi}{\mu} + \left( N_0 - \frac{\Pi}{\mu} \right) e^{-\mu t}, \quad N_0 = N(0),$$

which shows that the living population satisfies  $N(t) \leq \Pi/\mu$  as  $t \rightarrow \infty$ .

For the deceased compartment, we have

$$\frac{dD_c}{dt} = \delta I_c - \alpha D_c \leq \delta \frac{\Pi}{\mu} - \alpha D_c,$$

so that

$$D_c(t) \leq \frac{\delta}{\alpha} \cdot \frac{\Pi}{\mu} + \left( D_0 - \frac{\delta}{\alpha} \cdot \frac{\Pi}{\mu} \right) e^{-\alpha t}.$$

Consequently,

$$\mathcal{E}^0 = \left( \frac{\Pi}{\mu}, 0, 0, 0, 0 \right)$$

is the disease-free equilibrium (DFE).

*Next-Generation Matrix and the Basic Reproduction Number  $\mathcal{R}_{\mathcal{D}}$*  Consider the vector of infected compartments

$$X = (E_c, I_c, D_c)^T.$$

Following the standard next-generation approach [19,20,21], let  $F$  denote the matrix of new infection terms and  $V$  represent the matrix of transitions among infected compartments.

$FV^{-1}$  then results in the next-generation matrix:

$$FV^{-1} = \begin{pmatrix} \frac{\beta_1 \sigma}{(\mu + \sigma)(\mu + \gamma + \delta)} + \frac{\omega \beta_2 \sigma (\mu + \delta)}{(\mu + \sigma)(\mu + \gamma + \delta)\alpha} & \frac{\beta_1}{\gamma + \delta + \mu} + \frac{\omega \beta_2 \delta}{(\gamma + \delta + \mu)\alpha} & \frac{\omega \beta_2}{\alpha} \\ 0 & 0 & 0 \\ 0 & 0 & 0 \end{pmatrix}.$$

The spectral radius (dominant eigenvalue) of  $FV^{-1}$  represents the basic reproduction number  $\mathcal{R}_{\mathcal{D}}$ . On solving we get,

$$\mathcal{R}_{\mathcal{D}} = \frac{\sigma \beta_1}{(\mu + \sigma)(\mu + \gamma + \delta)} + \frac{\omega \beta_2 \sigma \delta}{(\mu + \sigma)(\mu + \gamma + \delta)\alpha}$$

$\mathcal{R}_{\mathcal{D}}$  gives the expected number of secondary infections which may be caused by a single infected person in a population that is fully susceptible [20].

*Interpretation:*

- If  $\mathcal{R}_{\mathcal{D}} < 1$ , the disease-free equilibrium is locally asymptotically stable.
- if  $\mathcal{R}_{\mathcal{D}} > 1$  then the disease-free equilibrium is unstable.

#### 4.2. Stability Analysis of the Disease-Free Equilibrium (DFE)

**Theorem 4.2** *The disease-free equilibrium (DFE) of system (3.1) is*

$$\mathcal{E}_0 = \left( \frac{\Pi}{\mu}, 0, 0, 0, 0 \right),$$

and it satisfies:

- (i) **Locally asymptotically stable** if  $\mathcal{R}_{\mathcal{D}} < 1$ ,
- (ii) **Unstable** if  $\mathcal{R}_{\mathcal{D}} > 1$ .

**Proof:** The local stability of  $\mathcal{E}_0$  is ascertained by the eigenvalues of the Jacobian matrix

$$J(\mathcal{E}_0) = \begin{pmatrix} -\mu & 0 & -\beta_1 & 0 & -\omega \beta_2 \\ 0 & -(\mu + \sigma) & \beta_1 & 0 & \omega \beta_2 \\ 0 & \sigma & -(\mu + \gamma + \delta) & 0 & 0 \\ 0 & 0 & \gamma & -\mu & 0 \\ 0 & 0 & \delta & 0 & -\alpha \end{pmatrix}.$$

The Jacobian has a block structure, so

$$\det(J(\mathcal{E}_0) - \lambda I) = (\lambda + \mu) \det(M - \lambda I) = 0,$$

where the  $3 \times 3$  infected subsystem  $(E_c, I_c, D_c)$  is

$$M = \begin{pmatrix} -(\mu + \sigma) & \beta_1 & \omega\beta_2 \\ \sigma & -(\mu + \gamma + \delta) & 0 \\ 0 & \delta & -\alpha \end{pmatrix}.$$

Two eigenvalues are

$$\lambda_1 = -\mu \quad (\text{negative}).$$

Thus, stability depends on the following cubic polynomial

$$P(\lambda) = \det(M - \lambda I) = \lambda^3 + a_1\lambda^2 + a_2\lambda + a_3.$$

where we define,

$$A = \mu + \sigma, \quad B = \mu + \gamma + \delta, \quad C = \alpha.$$

and

$$\begin{aligned} a_1 &= A + B + C > 0, \\ a_2 &= AB + AC + BC - \beta_1\sigma > 0 \quad (\text{for } \mathcal{R}_D < 1), \\ a_3 &= ABC - \beta_1\sigma C - \omega\beta_2\sigma\delta = ABC(1 - \mathcal{R}_D). \end{aligned}$$

The DFE is locally asymptotically stable given by Routh-Hurwitz criteria, if

$$a_1 > 0, \quad a_2 > 0, \quad a_3 > 0, \quad a_1a_2 - a_3 > 0.$$

For  $\mathcal{R}_D < 1$ ,  $a_3 > 0$ , and all other coefficients are positive. Therefore, all roots of  $P(\lambda)$  have negative real parts, and the DFE is locally asymptotically stable.

Hence, the disease-free equilibrium is locally asymptotically stable if and only if  $\mathcal{R}_D < 1$ , and unstable if  $\mathcal{R}_D > 1$ .  $\square$

### 4.3. Existence of Endemic Equilibrium

**Theorem 4.3** *If  $\mathcal{R}_D > 1$ , system (3.1) possesses a unique endemic equilibrium*

$$\mathcal{E}^* = (S_c^*, E_c^*, I_c^*, R_c^*, D_c^*),$$

where all components are strictly positive.

**Proof:** At equilibrium, all derivatives becomes zero. The force of infection is

$$\lambda = \frac{\beta_1 I_c^*}{N^*} + \frac{\omega\beta_2 D_c^*}{N^*}, \quad N^* = S_c^* + E_c^* + I_c^* + R_c^*.$$

The system at steady state gives:

$$\begin{aligned} 0 &= \Pi - \lambda S_c^* - \mu S_c^* + \theta R_c^*, \\ 0 &= \lambda S_c^* - (\mu + \sigma) E_c^*, \\ 0 &= \sigma E_c^* - (\mu + \gamma + \delta) I_c^*, \\ 0 &= \gamma I_c^* - (\mu + \theta) R_c^*, \\ 0 &= \delta I_c^* - \alpha D_c^*. \end{aligned}$$

From the last three equations, we obtain

$$E_c^* = \frac{\mu + \gamma + \delta}{\sigma} I_c^*, \quad R_c^* = \frac{\gamma}{\mu + \theta} I_c^*, \quad D_c^* = \frac{\delta}{\alpha} I_c^*.$$

The total living population at equilibrium is

$$N^* = S_c^* + E_c^* + I_c^* + R_c^* = S_c^* + \left( \frac{\mu + \gamma + \delta}{\sigma} + 1 + \frac{\gamma}{\mu + \theta} \right) I_c^*.$$

Define

$$\phi = \frac{\mu + \gamma + \delta}{\sigma} + 1 + \frac{\gamma}{\mu + \theta}, \quad \text{so that } N^* = S_c^* + \phi I_c^*.$$

The force of infection is

$$\lambda = \frac{\beta_1 I_c^* + \omega \beta_2 D_c^*}{N^*} = \frac{\beta_1 I_c^* + \omega \beta_2 \cdot \frac{\delta}{\alpha} I_c^*}{S_c^* + \phi I_c^*} = \frac{\Lambda I_c^*}{S_c^* + \phi I_c^*},$$

where

$$\Lambda = \beta_1 + \omega \beta_2 \cdot \frac{\delta}{\alpha}.$$

Substituting this into the equation for  $E_c^*$  gives

$$\frac{\Lambda I_c^*}{S_c^* + \phi I_c^*} \cdot S_c^* = (\mu + \sigma) E_c^* = (\mu + \sigma) \cdot \frac{\mu + \gamma + \delta}{\sigma} I_c^*.$$

Define

$$C = (\mu + \sigma) \cdot \frac{\mu + \gamma + \delta}{\sigma},$$

which results,

$$\frac{\Lambda S_c^*}{S_c^* + \phi I_c^*} = C \quad \implies \quad S_c^* = \frac{C \phi}{\Lambda - C} \cdot I_c^*.$$

Since  $I_c^* > 0$  at the endemic equilibrium by definition, we need  $S_c^* > 0$ . This holds if and only if  $\Lambda > C$ , or equivalently,

$$\mathcal{R}_D = \frac{\Lambda}{C} > 1.$$

Hence, a unique and biologically meaningful endemic equilibrium exists if and only if  $\mathcal{R}_D > 1$ .  $\square$

## 5. Global Stability of the Disease-Free Equilibrium

To determine the global asymptotic stability of the disease-free equilibrium (DFE)  $\mathcal{E}_0$ , LaSalle's Invariance Principle [22] is applied, and an appropriate Lyapunov function is constructed. At the disease-free equilibrium, the deceased compartment satisfies  $D_c=0$ . Hence, corpse-mediated transmission vanishes in a neighborhood of the DFE.

**Theorem 5.1** *If the basic reproduction number satisfies  $\mathcal{R}_D < 1$ , then the DFE  $\mathcal{E}_0$  of system (3.1) is globally asymptotically stable within the feasible domain  $\Omega$ .*

**Remark 5.1** This global stability result holds on the invariant set  $D_c = 0$ , where corpse-mediated transmission is absent.

**Proof:** Define the Lyapunov function

$$V = \sigma \alpha E_c + (\sigma + \mu) \alpha I_c.$$

Differentiating along system trajectories gives

$$\begin{aligned}\frac{dV}{dt} &= \sigma\alpha\frac{dE_c}{dt} + (\sigma + \mu)\alpha\frac{dI_c}{dt} \\ &= \sigma\alpha[\lambda S_c - (\sigma + \mu)E_c] + (\sigma + \mu)\alpha[\sigma E_c - (\mu + \gamma + \delta)I_c],\end{aligned}$$

where  $\lambda = \frac{\beta_1 I_c}{N}$ , as  $D_c = 0$  at the disease-free equilibrium.add this

The  $E_c$  terms cancel:

$$\frac{dV}{dt} = I_c[\sigma\alpha\beta_1 - (\sigma + \mu)\alpha(\mu + \gamma + \delta)].$$

Factor out the positive constant  $K = (\sigma + \mu)\alpha(\mu + \gamma + \delta)$ , and on the invariant set  $D_c = 0$ , corpse-mediated transmission is absent, and hence the basic reproduction number  $R_D$  reduces to its direct-transmission component  $\mathcal{R}_D = \frac{\sigma\beta_1}{(\mu + \sigma)(\mu + \gamma + \delta)}$  we get,

$$\frac{dV}{dt} = I_c K \left[ \frac{\sigma\beta_1}{(\sigma + \mu)(\mu + \gamma + \delta)} - 1 \right] = I_c K (\mathcal{R}_D - 1).$$

Since  $\mathcal{R}_D < 1$  by assumption,  $\frac{dV}{dt} < 0$  for all  $I_c > 0$ , and  $\frac{dV}{dt} = 0$  only at  $I_c = 0$ .

By LaSalle's invariance principle, all trajectories in  $\Omega$  converge to the largest invariant set where  $I_c = E_c = 0$ , which is exactly the DFE  $\mathcal{E}_0$ . Hence, the DFE is globally asymptotically stable.  $\square$

## 6. Numerical Simulations and Comparison

To evaluate the effect of corpse-mediated transmission, the SEIRD model is compared with the classical SEIR model studied by Lakshmi and Sabarmathi (2022) [14]. Although the SEIRD model includes additional parameters from the literature related to postmortem infectivity and corpse removal, the parameter values for the SEIR model are taken directly from their study.

For the SEIR model [14], the basic reproduction number is expressed as

$$\mathcal{R}_0^{SEIR} = \frac{\sigma\beta_1}{(\sigma + \mu)(\gamma + \mu)}. \quad (6.1)$$

In our SEIRD framework, which explicitly includes corpse-mediated transmission, the basic reproduction number becomes

$$\mathcal{R}_D^{SEIRD} = \frac{\sigma\beta_1}{(\sigma + \mu)(\gamma + \delta + \mu)} + \frac{\omega\beta_2\sigma\delta}{(\sigma + \mu)(\gamma + \delta + \mu)\alpha}. \quad (6.2)$$

For the numerical simulations, with  $N = 1000$  and  $I = 1$ , the following parameter values are used:

- $\beta_1 = 0.75$ ,  $\sigma = 0.1053$ ,  $\gamma = 0.1176$ ,  $\mu = 0.0189$  (from [14])
- $\delta = 0.76$ ,  $\beta_2 = 0.65$  (from [12])
- $\omega = 0.5$ ,  $\alpha = 0.6$  (assumed)

The SEIRD model decomposes  $\mathcal{R}_D$  into contributions from both direct infections and those arising from contact with unburied corpses, whereas the SEIR model considers only direct transmission. It is observed that the inclusion of corpse-mediated transmission significantly changes the epidemic dynamics. The predicted outbreak trajectories for the two models are presented in Figure 2 and Table 2. This explains the SEIRD model's delayed peak and lower total number of cases in comparison with the classical SEIR framework.

Table 2: Comparison of epidemic characteristics between SEIR and SEIRD models

Model	$R_0$	Peak $I$	Time to Peak (days)	Total Cases	Duration (days)
SEIR	4.658	191.9	28.6	146.5	100
SEIRD	1.108	9.3	36.6	15.5	100

The SEIR model predicts a substantially larger epidemic, with a peak of approximately 192 infectious individuals on day 28.6. Whereas the SEIRD model, in which corpse-mediated transmission is included, predicts a significantly smaller outbreak, with only 9.3 infectious individuals at the peak occurring later, on day 36.6. The total number of cases is also evidently reduced

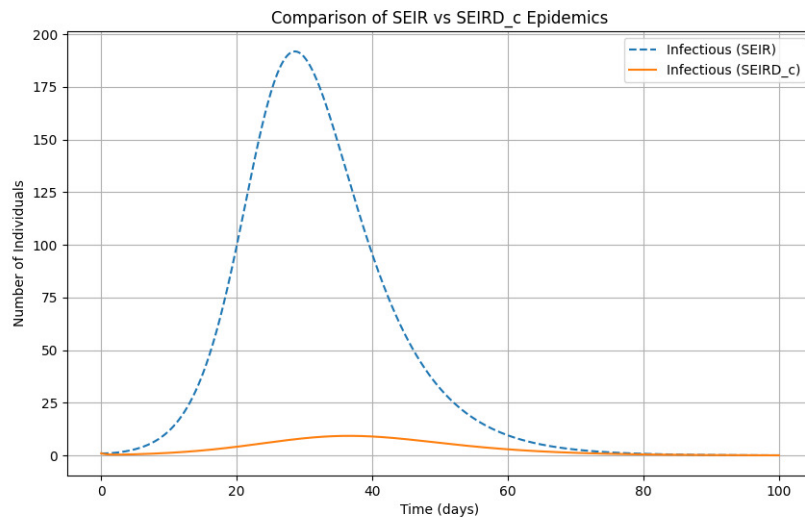


Figure 2: Comparison of infectious individuals  $I(t)$  between SEIR and SEIRD models.

## 7. Interpretation and Sensitivity Analysis of the SEIRD Model

System (3.1) has been numerically computed using Python's `odeint` routine (`scipy.integrate`), with the initial conditions and parameter values summarized in Table 3. The simulations have been performed over a time span of 60 days to investigate the time-based dynamics of the model. Please note that different parameter sets are used for comparative analysis in Section 6 and for sensitivity exploration in Section 7.

Symbol	Value	Reference
$S_c$	152.7 M	[12]
$E_c$	1 M	Assumed
$I_c$	0.1 M	Assumed
$R_c$	0	[12]
$D_c$	0.05 M	Assumed
$\sigma$	0.6 day <sup>-1</sup>	[12]
$\Pi$	62951 day <sup>-1</sup>	Assumed
$\beta_1$	0.75 day <sup>-1</sup>	[12]
$\beta_2$	0.65 day <sup>-1</sup>	[12]
$\mu$	$3.8642 \times 10^{-5}$ day <sup>-1</sup>	[12]
$\alpha$	0.5 day <sup>-1</sup>	Assumed
$\theta$	0.85 day <sup>-1</sup>	Assumed
$\omega$	0.5	Assumed
$\gamma$	0.09 day <sup>-1</sup>	[12]
$\delta$	0.76 day <sup>-1</sup>	[12]

Table 3: Summary of initial conditions and parameter values used in the SEIRD model for analyzing Nipah virus transmission dynamics.

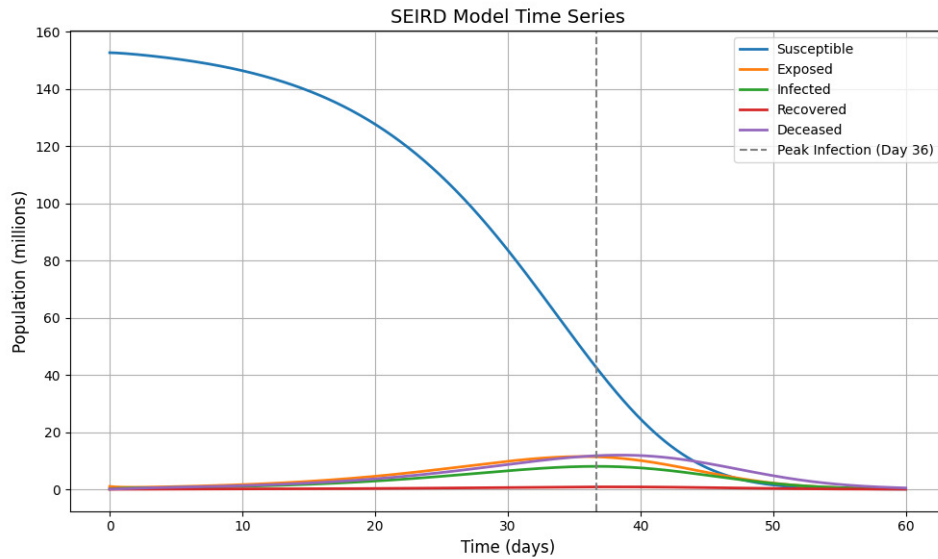


Figure 3: Dynamics of all SEIRD compartments ( $S_c$ ,  $E_c$ ,  $I_c$ ,  $R_c$ ,  $D_c$ ) over the course of the simulation.

Interpretation. In Figure 3,  $S_c$ , the number of susceptibles reduces rapidly, whereas  $E_c$  and  $I_c$  reach their peaks around day 30. After a delay, recoveries ( $R_c$ ) and deaths ( $D_c$ ) occur, and the system stabilizes by day 50. Controlling the outbreak requires an increase in the recovery rate ( $\gamma$ ) and a decrease in the transmission rates ( $\beta_1$ ,  $\beta_2$ ).

### 7.1. Sensitivity Analysis

Key parameters influencing  $I_c(t)$  include  $\beta_1$ ,  $\beta_2$ ,  $\omega$ ,  $\gamma$ , and  $\delta$ .

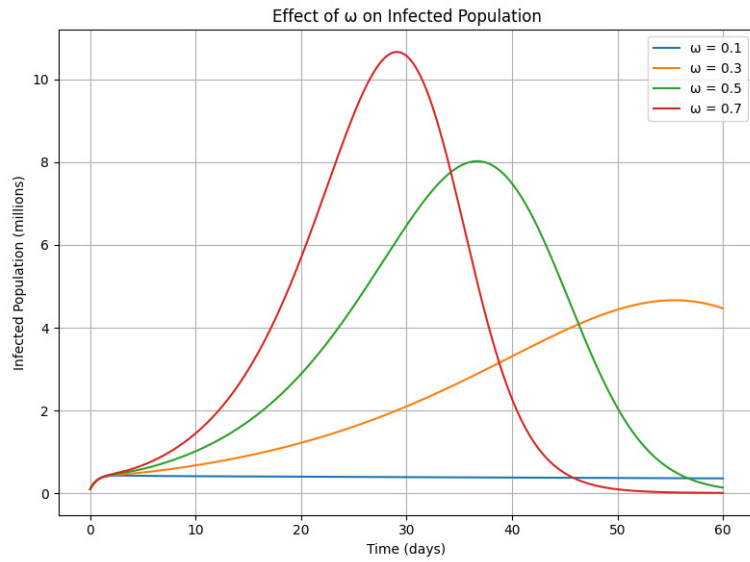


Figure 4: Impact of unsafe corpse handling  $\omega$  on  $I_c(t)$ .

*Sensitivity to Unsafe Corpse Handling  $\omega$*  The period of outbreaks and peak infections is increased by higher values of  $\omega$ , indicating that improper handling of corpses greatly increases transmission.

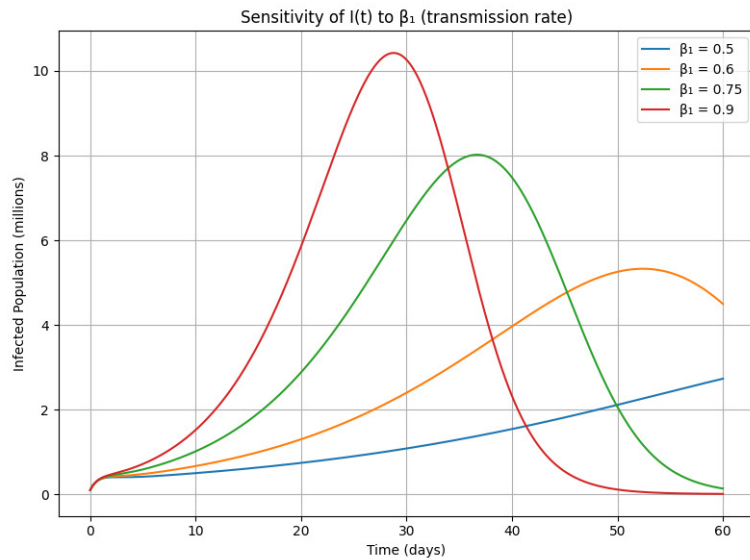


Figure 5: Impact of  $\beta_1$  on  $I_c(t)$ .

*Sensitivity to Transmission Rate  $\beta_1$*  The importance of interventions that reduce person-to-person contact is highlighted by the fact that increasing  $\beta_1$  accelerates the outbreak and raises the infection peak.

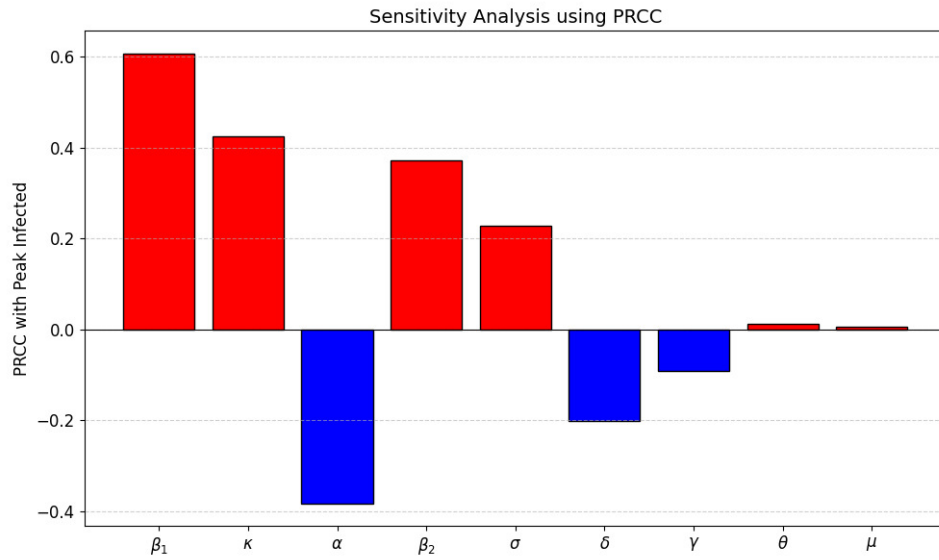


Figure 6: Partial rank correlation coefficients (PRCC) indicating parameter influence on peak infections.

*PRCC Sensitivity Analysis* Figure 6 shows that  $\omega$  and  $\beta_1$  have the most substantial positive effects on peak infections. Although the recovery rate ( $\gamma$ ) and natural mortality rate ( $\mu$ ) have a smaller impact, faster corpse management ( $\alpha$ ) reduces the peak number of cases.

## 7.2. Phase Plane Analysis

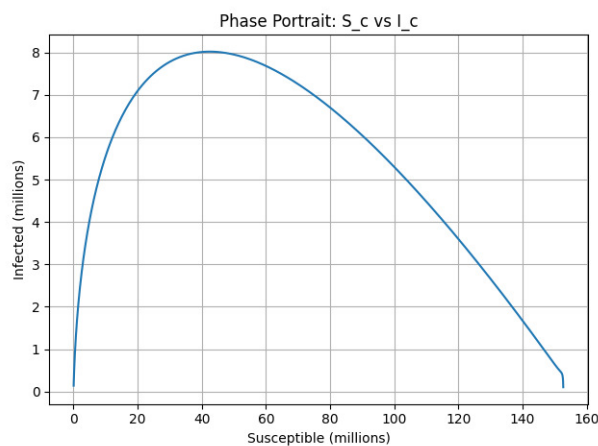


Figure 7: Phase portrait of  $S_c$  versus  $I_c$ .

When susceptibles are ample, the  $S_c$ - $I_c$  phase portrait illustrates rapid infection growth; however, as recoveries and deaths reduce the the number of susceptibles, the infection subsequently declines.

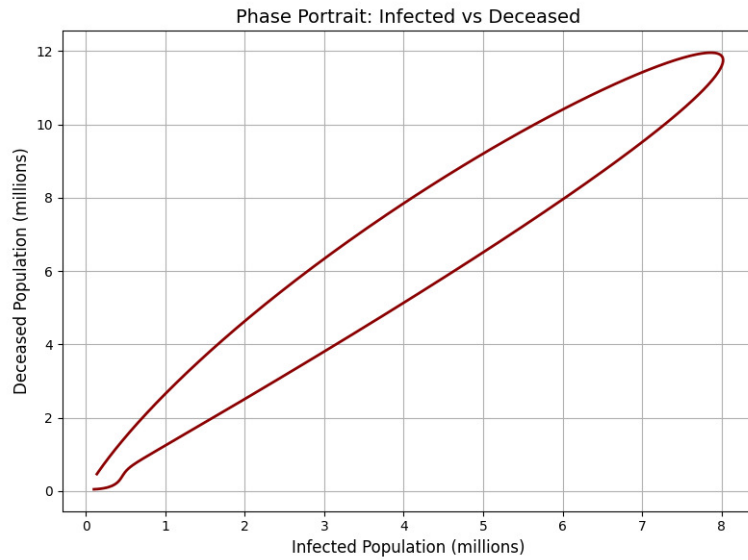


Figure 8: Phase portrait of  $I_c$  versus  $D_c$ .

As the epidemic declines, the  $I_c$ - $D_c$  phase portrait shows that the death toll slows and increases with infections.

### 8. Contour Plot of Reproduction Number $\mathcal{R}_D$

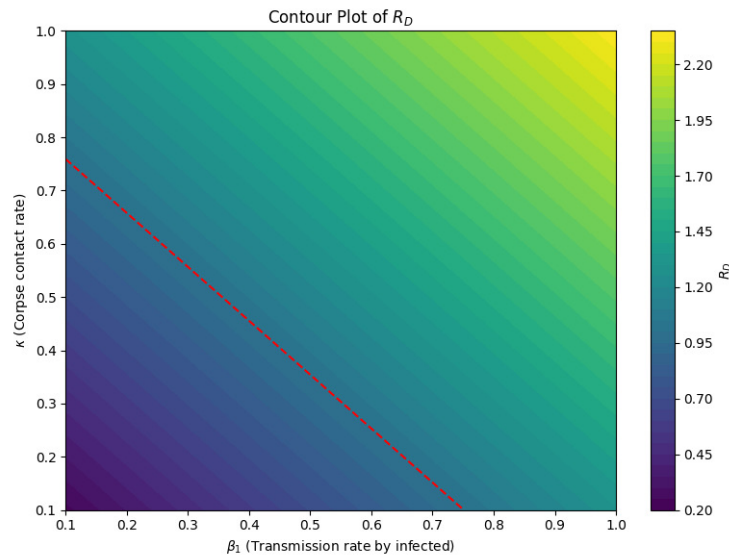


Figure 9: Contour of  $\mathcal{R}_D$  with respect to  $\beta_1$  and  $\omega$ . The dotted line indicates  $\mathcal{R}_D = 1$ .

The contour plot guides intervention strategies aimed at reducing outbreak potential by showing how combinations of  $\beta_1$  and  $\omega$  influence  $\mathcal{R}_D$ .

### 9. Conclusion

An SEIRD model for Nipah virus transmission, which includes five compartments—viz, susceptible, exposed, infectious, recovered, and deceased—is presented. This model explicitly considers corpse-

mediated infection. The system is stable when  $\mathcal{R}_D < 1$ , whereas a transition to an endemic state occurs when  $\mathcal{R}_D > 1$ . Analytical conditions for both the disease-free and endemic equilibria have been established. These theoretical findings have been supported by numerical simulations, which confirm that the most significant factors influencing outbreak dynamics are the transmission parameters ( $\beta_1, \beta_2$ ) and unsafe corpse handling ( $\omega$ ). Additionally, PRCC and sensitivity analyses indicate that increasing recovery rates or reducing transmission can substantially lessen the severity of an epidemic. Overall, the study highlights the critical importance of safe corpse handling and rapid interventions in reducing the death rate, flattening the epidemic curve, and easing the burden on healthcare systems.

## 10. Future Scope

The model can be further improved through several extensions to validate its practical applicability in real-world scenarios. Time-dependent parameters can be incorporated, quarantine or vaccination variables can be added, network- or area-wise assortment can be considered, and parameters can be validated using real NiV outbreak data. These extensions can help improve prediction accuracy and support better public health decision-making.

## References

1. M. S. Chadha, J. A. Comer, L. Lowe, P. A. Rota, P. E. Rollin, W. J. Bellini, T. G. Ksiazek, A. C. Mishra, *nipah virus-associated encephalitis outbreak, siliguri, india*, Emerg. Infect. Dis. 12, 235–240, (2006).
2. G. Arunkumar, R. Chandni, D. T. Mourya, S. K. Singh, R. Sadanandan, P. Sudan, *outbreak investigation of nipah virus disease in kerala, india, 2018*, J. Infect. Dis. 219, 1867–1878, (2019).
3. A. Lo Presti, E. Cella, M. Giovanetti, A. Lai, S. Angeletti, G. Zehender, *nipah virus: epidemiology, molecular determinants and future challenges*, Microbes Infect. 18, 848–859, (2016).
4. K. Halpin, A. D. Hyatt, R. Fogarty, D. Middleton, J. Bingham, J. H. Epstein, S. A. Rahman, T. Hughes, C. Smith, H. E. Field, *pteropid bats are confirmed as the reservoir hosts of henipaviruses: a comprehensive experimental study of virus transmission*, Am. J. Trop. Med. Hyg. 85, 946, (2011).
5. K. B. Chua, K. J. Goh, K. T. Wong, A. Kamarulzaman, P. S. K. Tan, T. G. Ksiazek, S. R. Zaki, G. Paul, S. K. Lam, C. T. Tan, *fatal encephalitis due to nipah virus among pig-farmers in malaysia*, Lancet 354, 1257–1259, (1999).
6. L. M. Looi, K. B. Chua, *nipah virus encephalitis: recent advances and remaining challenges*, J. Pathol. 212, 267–272, (2007).
7. S. P. Luby, E. S. Gurley, M. J. Hossain, *transmission of human infection with nipah virus*, Clin. Infect. Dis. 49, 1743–1748, (2009).
8. B. A. Clayton, D. Middleton, J. Bergfeld, L. F. Wang, *transmission routes for nipah virus from humans and bats: insights from outbreaks*, Curr. Opin. Virol. 45, 16–24, (2020).
9. M. Martcheva, *An Introduction to Mathematical Epidemiology*, Springer, (2015).
10. F. Brauer, C. Castillo-Chavez, *Mathematical Models in Epidemiology*, Springer, (2019).
11. W. O. Kermack, A. G. McKendrick, *a contribution to the mathematical theory of epidemics*, Proc. R. Soc. Lond. A 115, 700–721, (1927).
12. M. K. Mondal, M. Hanif, M. H. A. Biswas, *a mathematical analysis for controlling the spread of nipah virus infection*, Int. J. Model. Simul. 37, 185–197, (2017).
13. B. S. P. Ang, T. C. C. Lim, L. Wang, *nipah virus infection*, J. Clin. Microbiol. 56, e01875–17, (2018).
14. V. S. V. Naga Soundarya Lakshmi, A. Sabarmathi, *dynamics of seir model of nipah virus*, Recent Adv. Appl. Math. Dyn. Fluid Flows, 273–284, (2022).
15. A. D. Zewdie, S. Gakkhar, *a mathematical model for nipah virus infection*, J. Appl. Math. 2020, 1–10, (2020).
16. M. H. A. Biswas, *optimal control of nipah virus (niv) infections: a bangladesh scenario*, J. Pure Appl. Math. Adv. Appl. 12, 77–104, (2014).
17. J. Sultana, C. N. Podder, *mathematical analysis of nipah virus infections using optimal control theory*, J. Appl. Math. Phys. 4, 1099, (2016).
18. H. S. Nita, D. T. Niketa, A. T. Foram, H. S. Moksha, *control strategies for nipah virus*, Int. J. Appl. Eng. Res. 13, 15149–15163, (2018).
19. O. Diekmann, J. A. P. Heesterbeek, J. A. J. Metz, *on the definition and computation of the basic reproduction ratio  $R_0$  in models for infectious diseases in heterogeneous populations*, J. Math. Biol. 28, 365–382, (1990).
20. P. van den Driessche, J. Watmough, *reproduction numbers and sub-threshold endemic equilibria for compartmental models of disease transmission*, Math. Biosci. 180, 29–48, (2002).

21. J. A. P. Heesterbeek, *a brief history of  $R_0$  and a recipe for its calculation*, Acta Biotheor. 50, 189–204, (2002).
22. J. P. La Salle, *The Stability of Dynamical Systems*, SIAM, (1976).

*Mamta Kumari,*  
*DCT'S Dhempe College of Arts & Science,*  
*Panaji, Goa,*  
*India.*  
*E-mail address: [mamtakumarii2014@gmail.com](mailto:mamtakumarii2014@gmail.com)*